The Late Endosomal ClC-6 Mediates Proton/Chloride Countertransport in Heterologous Plasma Membrane Expression*[S]

Ioana Neagoe, Tobias Stauber, Pawel Fidzinski, Eun-Yeong Bergsdorf, and Thomas J. Jentsch[1]

From the Leibniz-Institut für Molekulare Pharmakologie (FMP) and Max-Delbrück-Centrum für Molekulare Medizin (MDC), D-13125 Berlin, Germany

Members of the CLC protein family of Cl^- channels and transporters display the remarkable ability to function as either chloride channels or Cl^-/H^+ antiporters. Due to the intracellular localization of ClC-6 and ClC-7, it has not yet been possible to study the biophysical properties of these members of the late endosomal/lysosomal CLC branch in heterologous expression. Whereas recent data suggest that ClC-7 functions as an antiporter, transport characteristics of ClC-6 have remained entirely unknown. Here, we report that fusing the green fluorescent protein (GFP) to the N terminus of ClC-6 increased its cell surface expression, allowing us to functionally characterize ClC-6. Compatible with ClC-6 mediating Cl^-/H^+ exchange, *Xenopus* oocytes expressing GFP-tagged ClC-6 alkalinized upon depolarization. This alkalinization was dependent on the presence of extracellular anions and could occur against an electrochemical proton gradient. As observed in other CLC exchangers, ClC-6-mediated H^+ transport was abolished by mutations in either the "gating" or "proton" glutamate. Overexpression of GFP-tagged ClC-6 in CHO cells elicited small, outwardly rectifying currents with a $Cl^- > I^-$ conductance sequence. Mutating the gating glutamate of ClC-6 yielded an ohmic anion conductance that was increased by additionally mutating the "anion-coordinating" tyrosine. Additionally changing the chloride-coordinating serine 157 to proline increased the NO_3^- conductance of this mutant. Taken together, these data demonstrate for the first time that ClC-6 is a Cl^-/H^+ antiporter.

The CLC gene family, originally thought to encode exclusively chloride channels, is now recognized to comprise both channels and anion-proton antiporters (1). Following the discovery that the bacterial EcClC-1 (one of the two CLC isoforms in *Escherichia coli*) functions as a $2Cl^-/H^+$ exchanger (2), mammalian endosomal ClC-4 and -5 were shown to mediate anion/proton exchange as well (3, 4). These endosomal electrogenic exchangers may facilitate endosomal acidification by shunting currents of the V-type ATPase and have a role in luminal Cl^- accumulation (5, 6). The plant AtClC-a functions phys-

iologically as an NO_3^-/H^+ exchanger that uses the pH gradient over the vacuole membrane to accumulate the nutrient NO_3^- into that organelle (7). With the notable exception of renal ClC-K channels (8), both channel- and exchanger-type CLC proteins share a glutamate in the permeation pathway that is involved in gating (in CLC channels) and in coupling chloride to proton countertransport (in CLC exchangers), respectively. Mutations in this gating glutamate profoundly affect CLC channel gating and uncouple anion from proton countertransport in CLC exchangers. All confirmed CLC antiporters display another glutamate (the proton glutamate) at their cytoplasmic surface that probably transfers protons to the central exchange site given by the gating glutamate (9–11). Because this proton glutamate is not found in confirmed CLC channels, its presence might indicate that the respective CLC is an exchanger.

Based on this hypothesis, ClC-3–7 should function as Cl^-/H^+ exchangers, but this remains to be shown for ClC-3, -6, and -7 by heterologous expression. Contrasting with ClC-4 and -5, which reach the plasma membrane to a degree that allows for detailed biophysical studies, currents mediated by ClC-3 were too low to determine whether it transports protons (3, 12). On the other hand, ClC-3 is ~80% identical in sequence to the established exchangers ClC-4 and ClC-5, with which it shares current properties that are similarly affected by mutations in the gating glutamate (12, 13). Hence, it is very likely that ClC-3 also functions as an exchanger. So far, it has been impossible to functionally express ClC-6 and ClC-7, which form a distinct branch of the CLC family (14), in the plasma membrane. This may be a consequence of their efficient targeting to late endosomes and lysosomes, respectively. ClC-7 is the only member of the CLC family significantly expressed on lysosomes (15–17). Lysosomes display $2Cl^-/H^+$ exchange activity (18, 19), which was strongly reduced by small interfering RNA in culture (18) and in ClC-7 knock-out (KO)[2] mice or ClC-7[unc] mice that carry an uncoupling mutation in the gating glutamate (19). Thus, there is no doubt that ClC-7 is a Cl^-/H^+ exchanger.

The functional properties of ClC-6, however, remain completely unknown. The ClC-6 protein is almost exclusively expressed in the nervous system where it localizes to late endosomes (20). The biological importance of ClC-6 is evident from KO mice, which display lysosomal storage disease that resem-

[S] The on-line version of this article (available at http://www.jbc.org) contains supplemental Figs. 1–3.
[1] To whom correspondence should be addressed: Leibniz-Institut für Molekulare Pharmakologie/Max-Delbrück-Centrum für Molekulare Medizin, Robert-Rössle-Str.10, D-13125 Berlin, Germany. Fax: 49-30-9406-2960; E-mail: Jentsch@fmp-berlin.de.

[2] The abbreviations used are: KO, knockout; BCECF, 2′,7′-bis(carboxyethyl)-5-(and-6)-carboxyfluorescein; DIDS, 4,4′-diisothiocyanatostilbene-2,2′-disulfonic acid; CHO, Chinese hamster ovary; GFP, green fluorescent protein; MES, 2-(*N*-morpholino)ethanesulfonic acid.

bles mild forms of human neuronal ceroid lipofuscinosis (20). Remarkably, this pathology is not associated with significant neuronal cell loss. A more severe form of lysosomal storage disease (and osteopetrosis) is observed with the loss of ClC-7 in mice and humans (15). A very similar phenotype is observed with the loss of Ostm1, an essential β-subunit of ClC-7 (21). Despite the belief that vesicular CLCs are generally involved in the acidification of intracellular organelles (22–24), lysosomal pH was normal in these KO mouse models (16, 20, 21). This observation led to the hypothesis (5) that these phenotypes are rather a consequence of impaired proton gradient-driven Cl^- accumulation in those vesicles, similar to impaired nitrate accumulation in plant vacuoles that lack AtClC-a (7). For ClC-7, this hypothesis is strongly supported by mice carrying an uncoupling point mutation in ClC-7. These mice accumulate less Cl^- in lysosomes and display severe lysosomal storage disease just like ClC-7 KO mice (19).

As the KO of ClC-6 also leads to lysosomal storage (20), it is of utmost importance to determine whether it likewise performs Cl^-/H^+ exchange. In this work, we achieve for the first time plasma membrane expression of wild-type and mutant ClC-6. We show unambiguously that ClC-6 mediates Cl^-/H^+ exchange and examine key mutants that change its coupling, conductance, and ion selectivity.

EXPERIMENTAL PROCEDURES

Expression Constructs—DNA-encoding human ClC-6 was cloned into the EcoRI site of pcDNA3 (Invitrogen) for expression in mammalian cells. For expression in *Xenopus* oocytes, ClC-6 was cloned into the pTLN vector (25). For expression of N-terminally GFP-tagged ClC-6 in mammalian cells, ClC-6-encoding DNA was inserted into pEGFP-C1 (Clontech) with the following linker sequence (including the initiator Met of ClC-6): SGLRSREFM. For the generation of the equivalent constructs for expression in *Xenopus* oocytes, EGFP was inserted first into pTLN (the resulting construct served as negative control), and subsequently, ClC-6 was inserted with the same linker sequence as in mammalian cell expression constructs. Point mutations were introduced by PCR with primers carrying the respective mutation. All constructs were confirmed by sequencing the complete open reading frame. The ClC-5 constructs have been described (26).

Electrophysiology and Qualitative pH_i Determinations—*Xenopus laevis* oocytes were injected with cRNA (5 ng for ClC-5 constructs and 30–35 ng for GFP and ClC-6 constructs) transcribed with the mMessage Machine kit (Ambion) according to the manufacturer's instructions after linearization of the plasmid with *Mlu*I. Currents were measured using standard two-electrode voltage clamp at room temperature employing a TurboTec10C amplifier (npi electronic (Gmbh)) and pClamp10 software (Molecular Devices).

Oocytes were superfused with modified ND96 saline (96 mM NaCl, 2 mM potassium gluconate, 1.8 mM calcium gluconate, 1 mM magnesium gluconate). pH was buffered with 5 mM HEPES, MES, or Tris as appropriate. Ion substitutions were done by replacing NaCl with equimolar amounts of $NaNO_3$ or NaI. Proton transport activity was measured with a fluorescence-based device called Fluorocyte (10) and allowed sensitive, qualitative

recording of intracellular pH (pH_i) changes based on the pH-sensitive excitation of BCECF (injected 10–30 min prior to the experiment). These measurements do not reflect pH_i averaged over the whole volume of the oocytes, but report pH_i changes close to the plasma membrane. Unless stated otherwise, the stimulation protocol consisted of depolarizing pulses to +90 mV for 400 ms interrupted by 100-ms pulses to −60 mV to avoid the activation of endogenous currents by prolonged depolarization (10). Current activation by standard two-electrode voltage clamp and pH_i changes were recorded simultaneously with the pClamp10 software. A relative measure of the alkalinization rate was determined semiquantitatively as the difference of the slopes of the normalized fluorescence values after and before the depolarization protocol.

Patch clamp measurements on CHO cells were performed by standard methods (27). Patch pipettes of 3–5 megohm resistance were filled with 110 mM CsCl, 8 mM NaCl, 0.5 mM $CaCl_2$, 1 mM EGTA, 2 mM Mg-ATP, 20 mM HEPES, pH 7.2. The calculated free Ca^{2+} concentration was 190 nM. The bath solution contained 118 mM NaCl, 5.6 mM KCl, 1 mM $MgCl_2$, 1 mM $CaCl_2$, 15 mM glucose, 5 mM HEPES, pH 7.5, with NaOH. Osmolarity was adjusted to 270 mosmol/kg for the pipette solution and 290 mosmol/kg for the extracellular solution by adding sucrose. Data were acquired with an EPC-10 double amplifier and Pulse software (HEKA). Whole-cell currents were measured by sequential 20-mV voltage steps from −100 to +100 mV. The Nernst equation ($V_{Nernst} = -RT/F \ln([Cl]_o/[Cl]_i)$) was used for reversal potential calculation. Reversal potentials measured with gluconate-containing solutions were corrected for liquid-junction potentials.

Surface Biotinylation—A membrane-impermeable NH_2-reactive biotin ester (sulfo-N-hydroxysuccinimide-LC-biotin; Pierce) was used to label plasma membrane proteins of *Xenopus* oocytes expressing ClC-6 constructs. Oocytes were incubated for 20 min at 4 °C in ND96 with 1 mg/ml biotin ester. After washing in ice-cold ND96, cells were homogenized in lysis buffer containing 150 mM NaCl, 20 mM Tris, pH 7.6, 1% Triton X-100, and protease inhibitor mixture (Complete+Pefa, Roche Applied Science). After centrifugation at 4000 × g for 1 min, the supernatant was precipitated with streptavidin beads (Pierce). Bound protein was eluted and separated by SDS-PAGE. For immunoblotting, we used rabbit antibodies directed against the C terminus of ClC-6 (6C3; supplemental Fig. 1) and actin (Sigma), respectively. Surface biotinylation of transfected CHO cells was performed similarly.

Immunofluorescence Microscopy—Plasmid DNA encoding the respective constructs was transfected using FuGENE6 (Roche Applied Science) according to the manufacturer's instructions, and cells were grown in a humidified 5% CO_2 incubator at 37 °C for a further 36 h before fixation with 4% paraformaldehyde in phosphate-buffered saline for 15 min. For immunostaining, cells were incubated with 30 mM glycine in phosphate-buffered saline for 5 min and permeabilized with 0.05% saponin in phosphate-buffered saline for 10 min. Both primary and Alexa Fluor-coupled secondary (Molecular Probes) antibodies were applied in phosphate-buffered saline/0.05% saponin supplemented with 3% bovine serum albumin. Untagged ClC-5 and ClC-6 were immunostained with rabbit
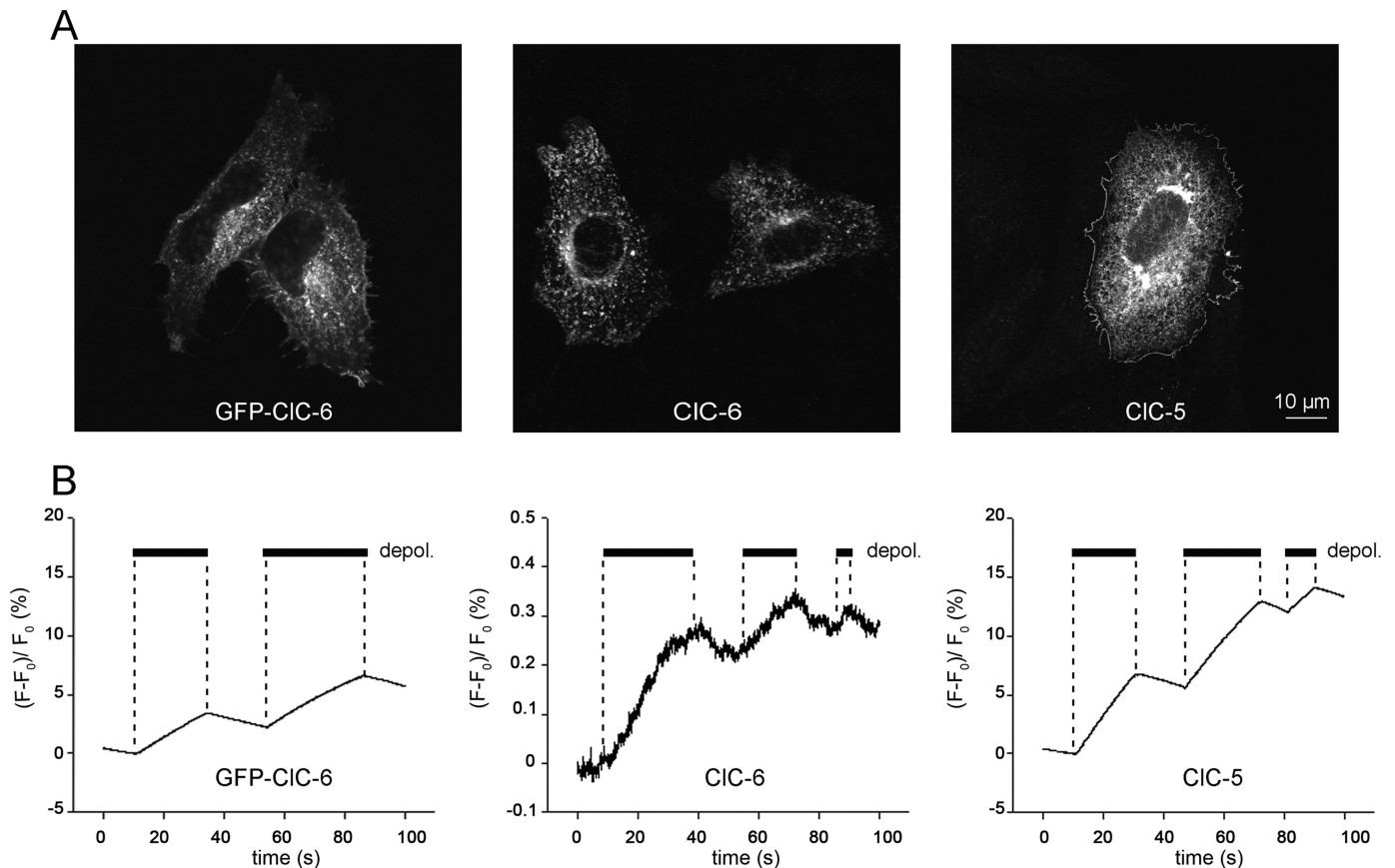
A

GFP-ClC-6   ClC-6   ClC-5   10 μm

B

FIGURE 1. **Plasma membrane-expressed ClC-6 functions as a proton transporter.** *A*, plasma membrane expression of GFP-ClC-6, ClC-6, and ClC-5 in CHO cells 36 h after transient transfection. The images show either the GFP signal (for GFP-ClC-6) or immunostaining signal for ClC-6 and ClC-5, respectively. *B*, voltage-driven H^+ transport in oocytes is shown for GFP-ClC-6, ClC-6, and ClC-5. Data are representative for GFP-ClC-6 ($n = 42$ from 21 batches of oocytes), for ClC-6 ($n = 9$ from 8 batches) and for ClC-5 ($n = 10$ from 5 batches). *Black bars* represent the length of the depolarization protocol (*depol.*), which consisted of pulses of 400 ms to $+90$ mV followed by 100 ms to -60 mV. The data represent change in BCECF fluorescence ($F - F_o$) normalized to the point before starting the depolarization protocol (F_0), qualitatively reflecting pH_i changes. The upward deflections correspond to intracellular alkalinization.

antibodies directed against the N terminus of ClC-5 (5A2) (28) and the C terminus of ClC-6 (6C3; supplemental Fig. 1), respectively. Images were acquired with an LSM510 laser scanning confocal microscope equipped with a 63×1.4 NA oil-immersion lens (Zeiss).

RESULTS

Previous attempts to record plasma membrane currents of ClC-6 have failed (14, 29) probably due to lack of insertion into the plasma membrane (20). When we expressed ClC-6 heterologously in mammalian cells, it localized predominantly to punctate intracellular structures and possibly to a very small extent to the plasma membrane (Fig. 1A). Agreeing with a previous study (30), heterologously expressed ClC-6 colocalized with markers of early and recycling endosomes (EEA1 and transferrin receptor, respectively) (data not shown). By contrast, native ClC-6 localizes to late endosomes of neuronal cells (20, 30). We observed that the fusion of GFP to the N terminus of ClC-6 increased its residence in the plasma membrane in several cell lines, including CHO cells (Fig. 1A), HeLa, HEK293, and COS7 cells (data not shown). GFP did not affect the localization of ClC-6 when fused to the C terminus of the protein (data not shown). A similar effect of an N-terminal GFP tag had been found previously for aquaporin 6. This water channel nor-

mally resides in intracellular compartments and is mislocalized to the plasma membrane with an N-terminal (but not with a C-terminal) GFP tag (31). The enhanced plasma membrane localization observed with the N-terminally tagged ClC-6, henceforth referred to as GFP-ClC-6, suggested that we might be able to study its biophysical properties at the plasma membrane.

We expressed this construct in oocytes from albino *Xenopus laevis* frogs and recorded simultaneously currents and changes in intracellular pH (pH_i) in response to changes in plasma membrane voltage. Currents were measured using the two-electrode voltage clamp technique. pH_i was measured qualitatively in our "Fluorocyte" device (10) that measures the pH-sensitive fluorescence of BCECF, with which oocytes had been injected before the experiment. While these nonratiometric measurements suffer invariably from a drift in fluorescence (10), it allows us to detect fluorescence changes induced by experimental maneuvers (*e.g.* depolarization) with extraordinary sensitivity. To minimize the activation of endogenous oocyte transport processes, oocytes were not depolarized continuously, but by a train of depolarizing pulses (3, 10). Whereas no currents above endogenous background levels were observed in oocytes expressing untagged ClC-6 or GFP-ClC-6,
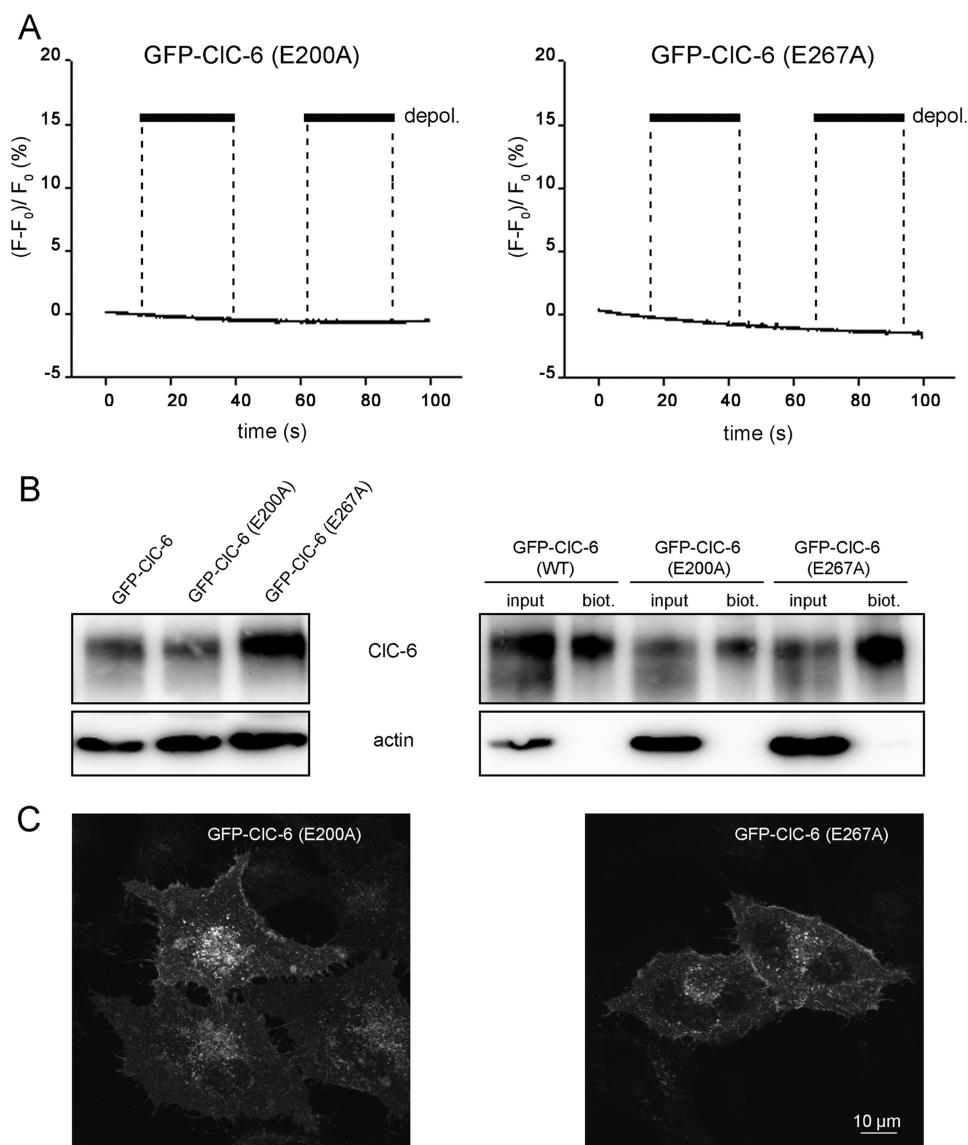
FIGURE 2. **Gating and proton glutamate mutations in GFP-ClC-6 abolish proton transport.** *A*, proton transport is abolished in both mutants. Data are representative for $n = 54$ from 11 batches for GFP-ClC6(E200A) and $n = 7$ from two batches for GFP-ClC-6(E267A). *B*, cell surface expression of GFP-ClC-6, GFP-ClC-6(E200A), and GFP-ClC-6(E267A) in injected *Xenopus* oocytes. Immunoblot of total protein (*left panel*) and cell surface-localized fractions (assayed by biotinylation; *right panel*) showed similar expression levels and cell surface localization for GFP-ClC-6 and the two mutants. The blots were tested for ClC-6 (antibody 6C3) and actin, respectively. *biot.*, biotinylated fraction. 3% of total protein was loaded as input. Surface biotinylation was quantified with transfected CHO cells. Normalized to relative surface expression of GFP-ClC-6, it yielded 0.82 ± 0.31 for GFP-ClC-6(E200A) and 2.44 ± 1.72 for GFP-ClC-6(E267A) ($\pm$ S.E., $n =$ five independent experiments). *C*, both constructs show plasma membrane localization upon heterologous expression in CHO cells. The images show GFP signal 36 h after transient transfection. *WT*, wild-type.

trains of depolarizing pulses (to $+90$ mV) induced cytosolic alkalinization (*i.e.* proton extrusion). Fig. 1*B* shows typical traces for GFP-ClC-6, ClC-6, and ClC-5. For ClC-5, both proton transport activity (Fig. 1*B*) and currents (data not shown) were detectable already after 2–3 days, whereas transport activity of GFP-ClC-6 became measurable only 5 days after cRNA injection. We also detected very weak depolarization-induced alkalinization in a few oocytes expressing wild-type ClC-6 (Fig. 1*B*). To ascertain that the observed pH$_i$ changes are mediated by GFP-ClC-6 rather than result from nonspecific activation of endogenous oocyte transporters (29), we inserted prototypical mutations into ClC-6 that are known to abolish proton trans-

port activity in established CLC antiporters. When either the gating or the proton glutamate of GFP-ClC-6 were mutated to alanine, depolarizing pulses no longer induced cytoplasmic alkalinization (Fig. 2*A*). This loss of H⁺ transport could not be attributed to reduced protein expression or diminished presence at the surface of oocytes (Fig. 2*B*). Likewise, the mutant proteins reached the plasma membrane in transfected mammalian cells (Fig. 2*C*). Hence, GFP-ClC-6 itself mediates proton transport.

As expected for a Cl⁻/H⁺ exchanger, replacing Cl⁻ with impermeable gluconate abolished depolarization-induced proton extrusion by both GFP-tagged (Fig. 3*A*) and untagged ClC-6 (supplemental Fig. 2). By contrast, proton extrusion was observed in the presence of external NO_3^- and I⁻, suggesting that GFP-ClC-6 can exchange these anions for protons (Fig. 3*B*). Unfortunately, the inability to record currents above background levels precluded the estimation of anion-to-proton coupling ratios. Depolarization-induced alkalinization occurred also against electrochemical proton gradients (Fig. 3*C*) in a direct demonstration of chloride-driven secondary active transport.

In the *Xenopus* expression system, determinations of pH$_i$ by the Fluorocyte device were more sensitive in detecting Cl⁻/H⁺ exchange (*i.e.* it suffered less from background problems) than measurements of electrical currents. To determine electrical properties of ClC-6 we therefore turned to other expression systems and tested several

mammalian cell lines for better signal-to-noise ratios. Surface expression of GFP-ClC-6 could be detected in several cell lines, including CHO (Fig. 1*A*). We finally chose CHO cells for expression as our previous study had shown that this cell line is virtually devoid of the Cl⁻/H⁺ exchanger ClC-5 (32), whose outwardly rectifying current may confound measurements of ClC-6, and because it displays low levels of other endogenous currents (27). Transient expression of GFP-ClC-6 in CHO cells resulted in currents that were significantly above background, although their magnitudes were low (Fig. 4*A*). These currents showed less outward rectification than ClC-5. As expected for a chloride conductance, replacing extracellular chloride with
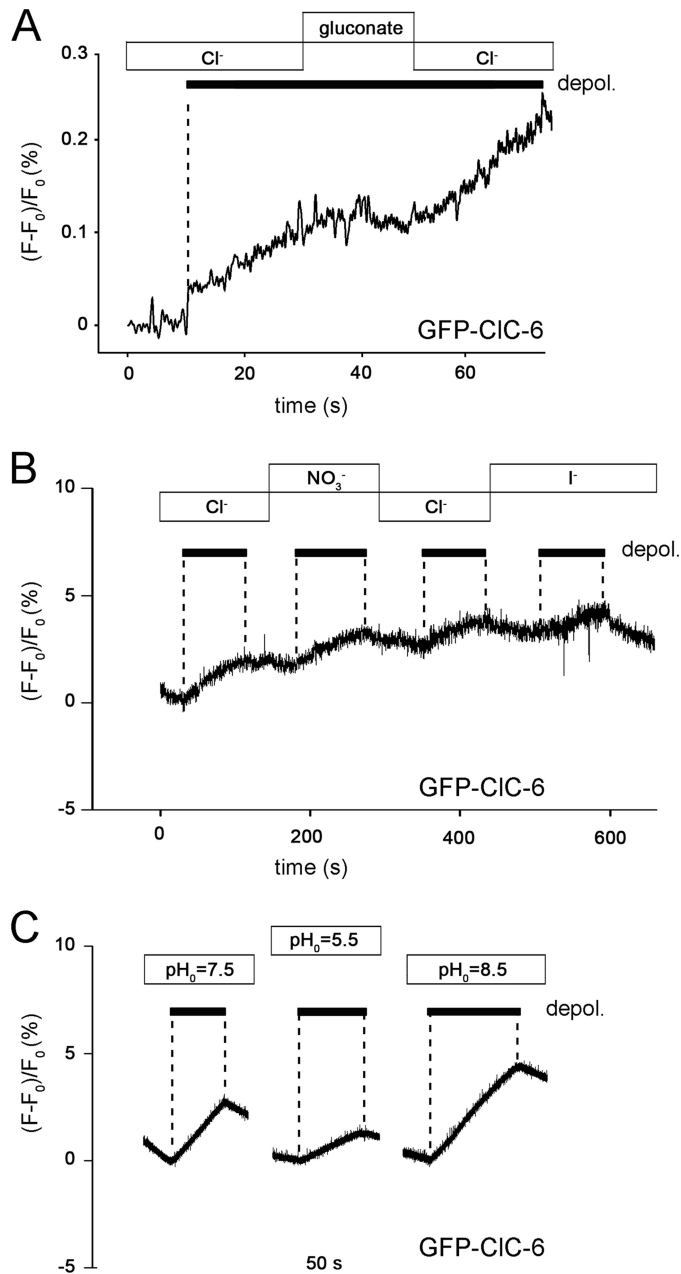
FIGURE 3. **Characterization of GFP-ClC-6- and ClC-6-mediated proton transport.** *A*, voltage-driven H^+ transport in oocytes expressing GFP-ClC-6 is chloride-dependent, as shown by the lack of alkalinization after replacing chloride with gluconate in the external solution. The rate of fluorescence (indicative of H^+ transport) change was 0.355 ± 0.084%/min with Cl^- and -0.004 ± 0.049%/min with gluconate ($n = 7$; $p < 0.001$), and 0.239 ± 0.030 after returning to Cl^- ($p < 0.01$ compared with gluconate). *B* and *C*, dependence of proton transport by GFP-ClC-6 on other extracellular anions replacing chloride (*B*) and on the extracellular pH (pH$_o$) (*C*). Similar effects were seen in $n = 8$ oocytes for ion substitution experiments similar to the one in *B* and $n = 20$ oocytes in *C*. Compared with values at pH$_o$ = 7.5, fluorescence changes were 54.7 ± 11.6% ($n = 12$, $p < 0.005$) and 145.2 ± 22.6% ($n = 5$; not significant) for pH$_o$ = 5.5 and 8.5, respectively (S.E., paired *t* test). Depolarization-driven proton transport was supported by chloride, iodide, and nitrate, but the low sensitivity of these qualitative measurements did not allow us to rank their potency in anion/proton exchange. All data (*A–C*) were recorded with oocytes superfused continuously with different external solutions. Depolarizing pulse trains (*depol.*) are represented by *black bars*; external solution exchange is represented by *rectangles*.

gluconate shifted the reversal potential to positive values (data not shown). Replacing chloride with other anions revealed a $Cl^- \sim NO_3^- > I^-$ conductance sequence (supplemental Fig. 3).

The low magnitudes of the currents and their rectification precluded a reasonably accurate determination of reversal potentials and permeability ratios. No currents could be elicited by the proton glutamate mutant E267A (Fig. 4*A*) and the gating glutamate mutant (E200A) yielded currents with a roughly linear current-voltage relationship (Fig. 4*B*), agreeing with the behavior of the equivalent ClC-5 mutant (10). The combination of two mutations in the bacterial EcClC-1 (E148A and Y445S) led to large, uncoupled anion currents (34). These mutations are thought to remove an external gate embodied by the gating glutamate and an internal gate represented by a Cl^--coordinating tyrosine. When we inserted equivalent mutations into GFP-ClC-6, the resulting mutant, GFP-ClC-6(E200A, Y576S), yielded currents that were about three times larger than those of the single gating glutamate (Fig. 4*B*), further supporting the notion that the observed currents are mediated by ClC-6. These currents showed both slight inward and outward rectification like those observed previously with gating glutamate mutations in ClC-4 and -5 (35). Extracellular application of the anion transport inhibitor DIDS (1 mM) nearly abolished the outwardly rectifying currents elicited by GFP-ClC-6 (Fig. 4*C*). As expected for a Cl^-/H^+ exchanger and similar to results obtained previously for ClC-4 and ClC-5 (35), extracellular alkalinization increased (Fig. 4*D*), whereas extracellular acidification decreased (Fig. 4*E*) GFP-ClC-6 currents. As expected with an uncoupling "gating glutamate" mutation, currents of the GFP-ClC-6(E200A, Y576S) were insensitive to changes in pH$_o$ (Fig. 4*F*). We neither detected proton transport with the Fluorocyte device when this mutant was expressed in *Xenopus* oocytes (data not shown). Unfortunately, the conductance of the outwardly rectifying GFP-ClC-6 was close to background conductance at the voltages where reversal potentials may be determined. We were therefore unable to reliably determine a shift in reversal potential with changes in extracellular pH, which is expected for Cl^-/H^+ exchangers (2). Although transfected CHO cells were suited to measure GFP-ClC-6-induced currents, our method to measure pH$_i$ changes with BCECF in cells depolarized using perforated patch-clamp technique (4) proved to be too insensitive to yield reliable results for GFP-ClC-6.

However, the increased current magnitudes of the GFP-ClC-6(E200A,Y576S) mutant allowed us to measure similar currents also in *Xenopus* oocytes (Fig. 5*A*). Ion substitution experiments revealed an $NO_3^- > Cl^- > I^-$ conductance sequence (Fig. 5*A*). In the presence of nitrate, the mutant protein showed outward rectification at positive potentials (Fig. 5, *A* and *B*). A similar change in rectification with nitrate had been observed previously in a gating glutamate mutant of ClC-5 (35). As expected for a pure anion conductance, substituting extracellular chloride for impermeable gluconate shifted the reversal potential to positive values according to the Nernst potential (Fig. 5*C*). To further substantiate that these currents were mediated by GFP-ClC-6(E200A,Y576S), we changed the Cl^--coordinating serine 157 to proline. Equivalent mutations in ClC-5 (11, 36), ClC-0 (11), and EcClC-1 (37) increased their preference for nitrate, whereas the inverse mutation decreased the relative nitrate conductance of the plant Cl^-/H^+ exchanger AtClC-a (11). The
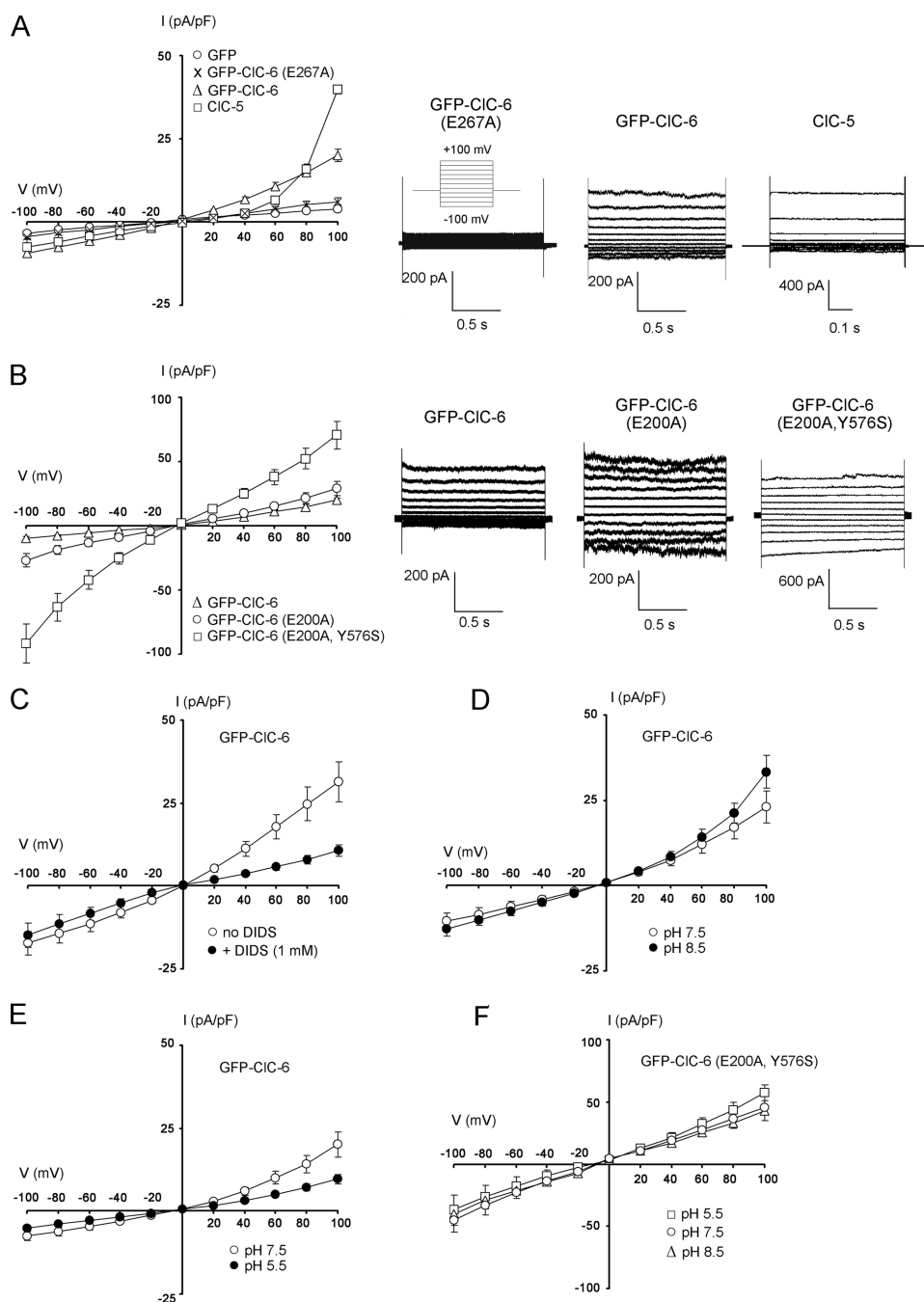
FIGURE 4. **GFP-ClC-6-mediated currents in CHO cells.** *A*, steady-state current/voltage curves and representative traces of GFP-ClC-6(E267A)-, GFP-ClC6- or ClC-5-transfected cells. In the *I/V* curve (*left*), GFP-injected oocytes are shown as an additional control. The mean ± S.E. of the current densities at +100 mV were 4.0 ± 0.5 pA/pF ($n = 20$, for GFP), 6.1 ± 1.2 pA/pF ($n = 13$, for GFP-ClC-6(E267A)), 20.0 ± 1.8 pA/pF ($n = 31$, for GFP-ClC-6) and 39.8 ± 1.3 pA/pF ($n = 5$, for ClC-5). *Inset*, the voltage-clamp protocol consisted of 20-mV steps to voltages between −100 and +100 mV for 2.2 s for ClC-6 constructs and 0.7 s for ClC-5. *B*, *I-V* curves and representative current traces of the gating glutamate mutant GFP-ClC-6(E200A) and the double mutant GFP-ClC-6(E200A,Y576S), which contains the additional mutation of the anion-coordinating tyrosine, in comparison with GFP-ClC-6 data (same as in *A*). The mean ± S.E. of the current densities at +100 mV were 29.2 ± 5.8 pA/pF ($n = 13$, for GFP-ClC-6(E200A)), 70.6 ± 10.8 pA/pF ($n = 23$, for GFP-ClC-6(E200A,Y576S)). *C*, effect of DIDS (1 mM) on currents elicited by GFP-ClC-6. Averaged currents from $n = 7$ cells before and after application of DIDS. *D* and *E*, pH dependence of GFP-ClC-6-mediated currents. Current-voltage relationships of individual transfected cells were measured with extracellular pH of 7.5, which was then changed to pH 8.5 (*D*, $n = 6$ cells) or pH 5.5 (*E*, $n = 9$ cells). The differences at voltages more positive than 40 mV were significant at the $p < 0.05$ level in paired t tests. *F*, currents mediated by GFP-ClC-6(E200A,Y576S) are insensitive to pH_o. The data represent mean ± S.E. of current densities for 16 cells.

triple mutant (S157P,E200A,Y576S) was compared with the starting construct GFP-ClC-6(E200A,Y576S) after transfection in CHO cells (Fig. 5, *D* and *E*). Patch clamp measurements in

the presence of different extracellular anions indeed showed that the S157P mutation increased the nitrate/chloride conductance ratio.

DISCUSSION

ClC-6 Is a Cl⁻/H⁺ Antiporter—We have recorded for the first time the transport activity of ClC-6. Using a fusion protein with enhanced surface expression and point mutations that changed transport properties in a manner that is typical for other CLC exchangers, we obtained compelling evidence that ClC-6 acts as an electrogenic anion/proton exchanger. Mutations of the gating and proton glutamates resulted in changes in charge and H⁺ transport that were similar to those found in other eukaryotic CLC exchangers (3, 4, 10, 11, 19). Moreover, the S157P mutant increased nitrate conductance of an uncoupled ClC-6 mutant. Taken together, the effects of these mutations very strongly bolster the conclusion that we have measured the transport activity of ClC-6 rather than transporters endogenous to the expression system.

To reach this conclusion, we had to resort to two different expression systems. *Xenopus* oocytes proved to be superior for the detection of small changes in pH_i resulting from proton transport, whereas exchanger currents could only be detected in transfected CHO cells. The detection of Cl⁻ currents in *Xenopus* oocytes is hampered by their large Ca²⁺-activated Cl⁻ conductance. Because the Fluorocyte measures pH_i close to the plasma membrane, the large volume of the oocytes does not preclude sensitive measurements of plasma membrane proton transport. Although the volume of CHO cells is much smaller than that of oocytes, even the perforated patch clamp technique we have used previously (4) does not totally prevent an equilibration of pH_i with the pH of the patch pipette.
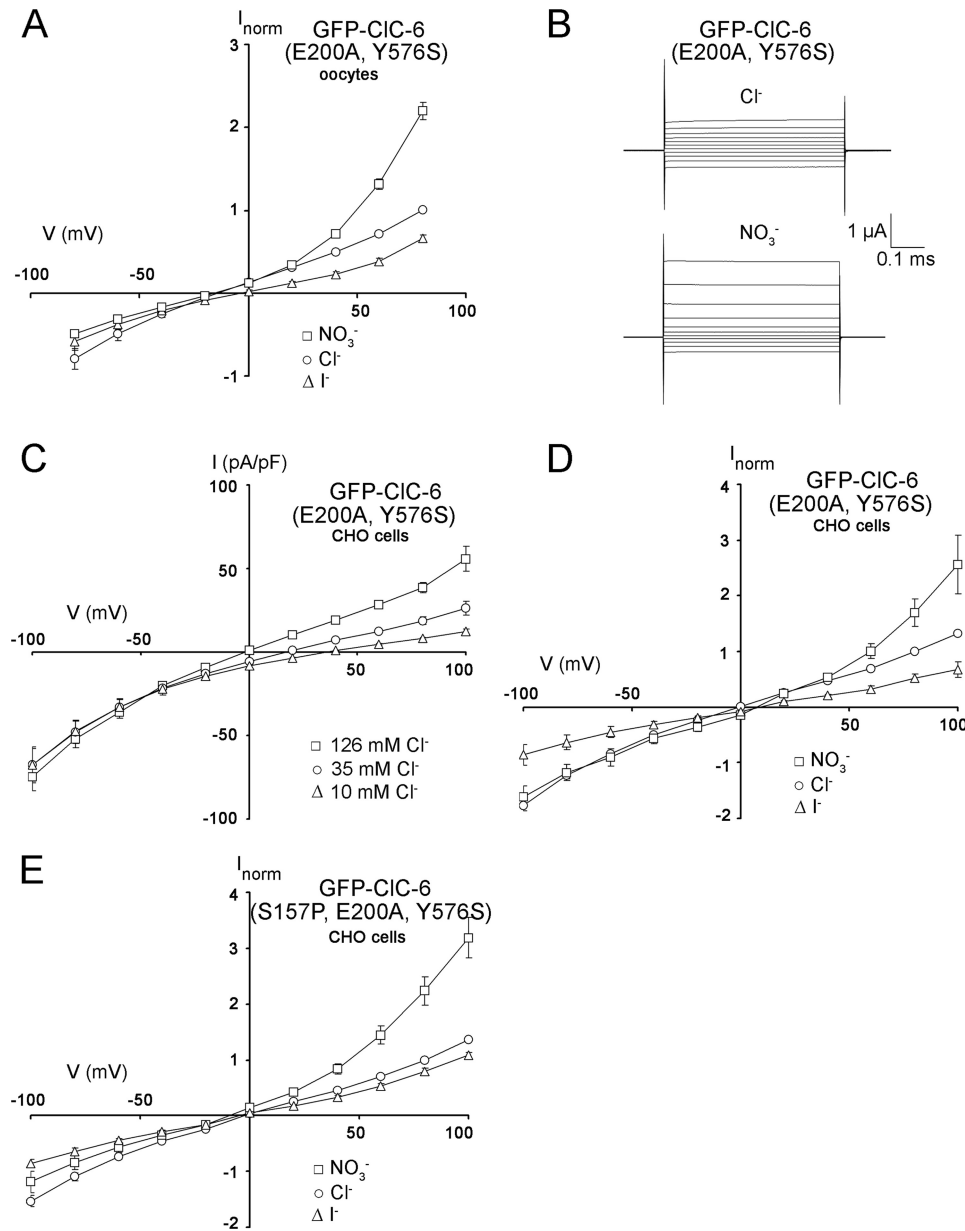
In most cases, we examined a GFP-ClC-6 fusion protein that yielded larger transport rates because of increased surface expression. We are confident that the measured transport qual-

FIGURE 5. **Biophysical characterization of GFP-ClC-6(E200A,Y576S) and GFP-ClC-6(S157P, E200A,Y576S) in *Xenopus* oocytes and CHO cells.** *A*, expression of GFP-ClC-6(E200A,Y576S) in oocytes induced linear currents with an $NO_3^- > Cl^- > I^-$ conductance sequence. Currents of 9–27 oocytes were normalized to the amplitude at +80 mV in Cl^- (with 2.69 ± 0.52 μA). *B*, representative voltage-clamp traces of an oocyte expressing GFP-ClC-6(E200A,Y576S) superfused with either Cl^- (*upper panel*) or NO_3^- (*lower panel*). *C*, GFP-ClC-6(E200A,Y576S)-transfected CHO cells were recorded in the presence of different extracellular chloride concentrations. When corrected for liquid junction potentials, the shift of reversal potential (given in mV) closely followed the calculated Nernst potentials: −6.9 ± 1.3 for 126 mM $[Cl^-]_o$ ($V_{Nernst} = -6.8$), 24 ± 1.9 for 35 mM $[Cl^-]_o$ ($V_{Nernst} = 26.5$), and 52.2 ± 1.9 for 10 mM $[Cl^-]_o$ ($V_{Nernst} = 56.5$). The data represent mean ± S.E. of current densities for 9–10 cells. *D*, CHO cells transfected with GFP-ClC-6(E200A,Y576S) were recorded in the presence of different extracellular anions. Current densities of 5–7 cells were normalized to the value at +80 mV in Cl^- (31.1 ± 4.6 pA/pF). The normalized value for NO_3^- was 1.7 ± 0.2 at +80 mV (current density 48.0 ± 7.3 pA/pF). *E*, Current densities of 7–11 CHO cells transfected with GFP-ClC-6(S157P,E200A,Y576S) were recorded in the presence of different extracellular anions and normalized to the value at +80 mV in Cl^- (25.9 ± 5.0 pA/pF). The normalized value in NO_3^- at +80 mV was 2.2 ± 0.2 (current density 62.4 ± 6.7pA/pF).

observe very small, but similar depolarization-induced alkalinization in a few oocytes overexpressing wild-type ClC-6.

In many respects, the transport properties of ClC-6 resembled those of other eukaryotic CLC exchangers. GFP-ClC-6 transport depended on the presence of anions. It displayed tight anion-proton coupling as demonstrated by its ability to transport protons against an electrochemical gradient. Proton transport could also be observed when chloride was replaced with iodide or nitrate ions that partially uncouple other CLC exchangers (10, 11, 38). Unfortunately, the low surface expression levels even of GFP-ClC-6 precluded the determination of coupling ratios. Therefore, we cannot make any statement as to a partial uncoupling of anion from proton fluxes with those ions. Like other CLC exchangers and channels, ClC-6 displayed a higher conductance with Cl^- than with I^-. In contrast to mammalian ClC-4 and -5 and to plant AtClC-a, nitrate conductance did not seem larger than chloride conductance. However, this observation must be viewed with caution because of the low expression levels. Rather unexpectedly, we found that 1 mM DIDS strongly inhibited GFP-ClC-6 currents. This contrasts with the insensitivity of ClC-5 to that anion transport inhibitor (32).

In addition to demonstrating that the observed transport activity is mediated by ClC-6, the present mutations in the ClC-6 backbone underpin the importance of certain key residues for Cl^-/H^+ exchange activity and selectivity. Just as in other CLC antiporters, neutralizing the gating glutamate converted ClC-6 into a pure anion conductance that was uncoupled from protons. Likewise, this mutation changed its voltage dependence to a slight inward and outward rectification like equivalent mutations in ClC-4 and -5 (4, 35). Neutralizing the proton glutamate suppressed both currents and H^+ transport below detection limits, similar to equivalent mutations in ClC-4 and -5 (3, 4) but contrasting with the corresponding EcClC-1 mutant that displayed uncoupled Cl^- transport

itatively reflects that of native ClC-6 because a) we did not observe changes in ClC-5 transport properties when it was tagged with GFP at its amino terminus,[3] and b) we could

---

[3] G. Rickheit and T. J. Jentsch, unpublished data.

(9). This loss of function could not be attributed to a decreased plasma membrane expression. We additionally mutated both the gating glutamate and a tyrosine that is involved in coordinating a chloride ion in the central binding site of EcClC-1 (39). These amino acids were hypothesized to form external and internal gates that open alternatively during exchange cycles. In support of this hypothesis, EcClC-1 showed largely increased transport rates in the (E148A,Y445S) double mutant (34). We tested this idea for the first time for a eukaryotic CLC exchanger. In ClC-6, the combination of these mutations also increased currents, albeit only by a factor of three compared with the single gating glutamate mutant. Based on the moderate increase in currents with the double mutant, we hesitate to call it "channel-like," as has been proposed for the equivalent EcClC-1 mutant (34). Finally, we showed that in the background of this double mutant an exchange of the Cl^--coordinating serine for proline increased its NO_3^- conductance. This result extends previous observations with ClC-5 (11, 36), ClC-0, and AtClC-a (11) as well as EcClC-1 (37) that a proline exchange at this position enhances nitrate selectivity. It also agrees with the earlier observation that even the conservative mutation of Ser¹²³-to-Thr changed the halide selectivity of ClC-0 (40). We conclude that this residue is a critical determinant of ion selectivity in both CLC channels and exchangers.

Currents recorded from GFP-ClC-6-transfected CHO cells were outwardly rectifying. Although the low signal-to-background ratio of these currents warrants a cautious interpretation, their rectification seemed less pronounced than those of ClC-3 to ClC-5 (3, 4, 27, 32, 35). AtClC-a also shows less rectification than those channels, both in plant vacuoles (7) and upon heterologous plasma membrane expression in *Xenopus* oocytes (11). No firm conclusion can be drawn about EcClC-1 and ClC-7 (2, 18, 19). The rectification of intracellular CLC transporters is of critical importance for understanding their role in intracellular organelles, which are mostly believed to be inside-positive.

Cell Biological Implications—Intracellular CLCs are thought to form functional modules with the vesicular H^+-ATPase. These vesicular CLCs may provide counterion conductances for electrogenic proton pumping, thereby facilitating acidification of the respective compartment. Indeed, ClC-3, -4, and -5 have been shown to be required for proper acidification of endosomes (6, 22–24, 41). The severe reduction in renal endocytosis observed with a loss of ClC-5 function may be attributed to reduced endosomal acidification (33) or Cl^- accumulation (6).

The disruption of ClC-6 or ClC-7/Ostm1 leads to lysosomal storage disease in the presence of normal lysosomal pH, which was carefully evaluated with ratiometric fluorescence measurements (16, 19–21). After the surprising finding that ClC-4 and ClC-5 actually mediate Cl^-/H^+ exchange rather than pure Cl^- conductance (3, 4), it has been speculated that intracellular CLCs in general may not only provide countercurrents for proton pumping but may increase the luminal chloride concentration in exchange for protons by secondary active transport. Supporting this hypothesis, organellar nitrate accrual has recently been shown for the plant CLC AtClC-a (7), and lysosomal Cl^- accumulation has been shown for ClC-7 (19).

In the present work, we have provided compelling evidence that ClC-6 functions as a Cl^-/H^+ exchanger and have used mutagenesis to show that its transport properties rely on certain key residues in a fashion similar to other CLC antiporters. Together with previous work (3, 4, 19), the present results suggest that all mammalian vesicular CLCs function as anion-proton antiporters and may have a dual role in vesicular acidification and chloride accumulation. Similar to lysosomal Cl^- accumulation by ClC-7 (19), ClC-6 may raise late endosomal Cl^- by taking it up in exchange for H^+. The lysosomal storage disease of ClC-6 KO mice (20) might be due to a reduced Cl^- concentration in late endosomes.

REFERENCES

1. Jentsch, T. J. (2008) *Crit. Rev. Biochem. Mol. Biol.* **43,** 3–36
2. Accardi, A., and Miller, C. (2004) *Nature* **427,** 803–807
3. Picollo, A., and Pusch, M. (2005) *Nature* **436,** 420–423
4. Scheel, O., Zdebik, A. A., Lourdel, S., and Jentsch, T. J. (2005) *Nature* **436,** 424–427
5. Jentsch, T. J. (2007) *J. Physiol.* **578,** 633–640
6. Novarino, G., Weinert, S., Rickheit, G., and Jentsch, T. J. (2010) *Science*, in press
7. De Angeli, A., Monachello, D., Ephritikhine, G., Frachisse, J. M., Thomine, S., Gambale, F., and Barbier-Brygoo, H. (2006) *Nature* **442,** 939–942
8. Kieferle, S., Fong, P., Bens, M., Vandewalle, A., and Jentsch, T. J. (1994) *Proc. Natl. Acad. Sci. U.S.A.* **91,** 6943–6947
9. Accardi, A., Walden, M., Nguitragool, W., Jayaram, H., Williams, C., and Miller, C. (2005) *J. Gen. Physiol.* **126,** 563–570
10. Zdebik, A. A., Zifarelli, G., Bergsdorf, E. Y., Soliani, P., Scheel, O., Jentsch, T. J., and Pusch, M. (2008) *J. Biol. Chem.* **283,** 4219–4227
11. Bergsdorf, E. Y., Zdebik, A. A., and Jentsch, T. J. (2009) *J. Biol. Chem.* **284,** 11184–11193
12. Matsuda, J. J., Filali, M. S., Volk, K. A., Collins, M. M., Moreland, J. G., and Lamb, F. S. (2008) *Am. J. Physiol. Cell Physiol* **294,** C251–262
13. Li, X., Wang, T., Zhao, Z., and Weinman, S. A. (2002) *Am. J. Physiol. Cell Physiol* **282,** C1483–1491
14. Brandt, S., and Jentsch, T. J. (1995) *FEBS Lett.* **377,** 15–20
15. Kornak, U., Kasper, D., Bösl, M. R., Kaiser, E., Schweizer, M., Schulz, A., Friedrich, W., Delling, G., and Jentsch, T. J. (2001) *Cell* **104,** 205–215
16. Kasper, D., Planells-Cases, R., Fuhrmann, J. C., Scheel, O., Zeitz, O., Ruether, K., Schmitt, A., Poët, M., Steinfeld, R., Schweizer, M., Kornak, U., and Jentsch, T. J. (2005) *EMBO J.* **24,** 1079–1091
17. Suzuki, T., Rai, T., Hayama, A., Sohara, E., Suda, S., Itoh, T., Sasaki, S., and Uchida, S. (2006) *J. Cell Physiol.* **206,** 792–798
18. Graves, A. R., Curran, P. K., Smith, C. L., and Mindell, J. A. (2008) *Nature* **453,** 788–792
19. Weinert, S., Jabs, S., Supanchart, C., Schweizer, M., Gimber, N., Richter, M., Rademann, J., Stauber, T., Kornak, U., and Jentsch, T. J. (2010) *Science*, in press
20. Poët, M., Kornak, U., Schweizer, M., Zdebik, A. A., Scheel, O., Hoelter, S., Wurst, W., Schmitt, A., Fuhrmann, J. C., Planells-Cases, R., Mole, S. E., Hübner, C. A., and Jentsch, T. J. (2006) *Proc. Natl. Acad. Sci. U.S.A.* **103,** 13854–13859
21. Lange, P. F., Wartosch, L., Jentsch, T. J., and Fuhrmann, J. C. (2006) *Nature* **440,** 220–223
22. Günther, W., Piwon, N., and Jentsch, T. J. (2003) *Pflügers Arch.* **445,** 456–462
23. Hara-Chikuma, M., Wang, Y., Guggino, S. E., Guggino, W. B., and Verk-

man, A. S. (2005) *Biochem. Biophys. Res. Commun.* **329,** 941–946

24. Hara-Chikuma, M., Yang, B., Sonawane, N. D., Sasaki, S., Uchida, S., and Verkman, A. S. (2005) *J. Biol. Chem.* **280,** 1241–1247
25. Lorenz, C., Pusch, M., and Jentsch, T. J. (1996) *Proc. Natl. Acad. Sci. U.S.A.* **93,** 13362–13366
26. Schwake, M., Friedrich, T., and Jentsch, T. J. (2001) *J. Biol. Chem.* **276,** 12049–12054
27. Li, X., Shimada, K., Showalter, L. A., and Weinman, S. A. (2000) *J. Biol. Chem.* **275,** 35994–35998
28. Günther, W., Lüchow, A., Cluzeaud, F., Vandewalle, A., and Jentsch, T. J. (1998) *Proc. Natl. Acad. Sci. U.S.A.* **95,** 8075–8080
29. Buyse, G., Voets, T., Tytgat, J., De Greef, C., Droogmans, G., Nilius, B., and Eggermont, J. (1997) *J. Biol. Chem.* **272,** 3615–3621
30. Ignoul, S., Simaels, J., Hermans, D., Annaert, W., and Eggermont, J. (2007) *PLoS ONE* **2,** e474
31. Beitz, E., Liu, K., Ikeda, M., Guggino, W. B., Agre, P., and Yasui, M. (2006) *Biol. Cell* **98,** 101–109
32. Steinmeyer, K., Schwappach, B., Bens, M., Vandewalle, A., and Jentsch, T. J. (1995) *J. Biol. Chem.* **270,** 31172–31177
33. Piwon, N., Günther, W., Schwake, M., Bösl, M. R., and Jentsch, T. J. (2000) *Nature* **408,** 369–373
34. Jayaram, H., Accardi, A., Wu, F., Williams, C., and Miller, C. (2008) *Proc. Natl. Acad. Sci. U.S.A.* **105,** 11194–11199
35. Friedrich, T., Breiderhoff, T., and Jentsch, T. J. (1999) *J. Biol. Chem.* **274,** 896–902
36. Zifarelli, G., and Pusch, M. (2009) *EMBO J.* **28,** 175–182
37. Picollo, A., Malvezzi, M., Houtman, J. C., and Accardi, A. (2009) *Nat. Struct. Mol. Biol.* **16,** 1294–1301
38. Nguitragool, W., and Miller, C. (2006) *J. Mol. Biol.* **362,** 682–690
39. Dutzler, R., Campbell, E. B., Cadene, M., Chait, B. T., and MacKinnon, R. (2002) *Nature* **415,** 287–294
40. Ludewig, U., Pusch, M., and Jentsch, T. J. (1996) *Nature* **383,** 340–343
41. Mohammad-Panah, R., Harrison, R., Dhani, S., Ackerley, C., Huan, L. J., Wang, Y., and Bear, C. E. (2003) *J. Biol. Chem.* **278,** 29267–29277